

ARTICLES

Polymer-Controlled Crystallization of Zinc Oxide Hexagonal Nanorings and Disks

Yin Peng,[†] An-Wu Xu,^{*,†,‡} Bin Deng,[†] Markus Antonietti,[‡] and Helmut Cölfen^{*,‡}*School of Chemistry and Chemical Engineering, Sun Yat-Sen University, Guangzhou 510275, China, and Max Planck Institute of Colloids and Interfaces, Department of Colloid Chemistry, MPI Research Campus Golm, 14424 Potsdam, Germany**Received: October 30, 2005; In Final Form: December 19, 2005*

In this study, we have developed a novel route to the synthesis of ZnO nanorings, disks, and diskoidlike crystals on a large scale by a facile solution-based method by using polymers as crystal growth modifiers. The crystals precipitated with polyacrylamide (PAM) as the additive show ringlike morphology. A possible growth mechanism of the ZnO nanostructures based on typical polymer–crystals interactions in a mild aqueous solution is given. The polymer contains in the side chain a large number of amide ligands that are able to coordinate with Zn^{2+} ions, that is, the otherwise just weakly exposed (001) face, leading to a lowering of surface energy and inhibition of growth along this direction and the formation of ringlike morphologies. While in the presence of carboxyl-functionalized polyacrylamide (PAM-COOH), nearly monodispersed disklike crystals were observed and finally evolved into diskoidlike microstructures with the reaction time prolonged. Polymer-directed crystal growth and mediated self-assembly of nanocrystals may provide promising routes to rational synthesis of various ordered inorganic and inorganic–organic hybrid materials with complex form and structural specialization.

Introduction

Control over crystallization is one of the most important techniques in modern materials science due to its potential to produce well-defined particles with unique structures in the nanometer and micrometer range. As nucleation and growth are highly sensitive processes, crystallization is usually controlled by various additives. Several groups have investigated the effect of biopolymers, synthetic macromolecules, supramolecular assemblies such as Langmuir monolayers, low-molecular-weight compounds, and others on the crystallization of CaCO_3 , BaSO_4 , and other inorganic minerals from solution under mild conditions.¹ These studies demonstrated the wide range of applications of additive and template-controlled crystallization for producing crystals with controlled structures in the presence of polymeric additives. Basic concepts in the study of biomineralization concern the use of organized biomolecules to exert precise control over the nucleation and growth, the shape and size, and the assembly of inorganic materials through organic and inorganic cooperative interaction at the inorganic and organic interface.^{2,3}

ZnO, as an important functional oxide, is a direct wide band gap (3.37 eV) semiconducting and piezoelectric material having many useful properties, such as optical absorption and emission, conductivity, piezoelectricity, photocatalysis, and sensitivity to

gases. The reports of ZnO nanobelts and nanolasers have aroused much interest in studies on the novel ZnO nanostructure fabrication and their applications.⁴ It is well documented that the shape and size of inorganic nanocrystals can control their widely changing optoelectronic and chemical properties. In this regard, it can be expected that some other novel morphologies for ZnO crystals would be promising candidates for room-temperature UV laser utilization or other interesting applications.

Different methods such as vapor–liquid–solid growth, thermal evaporation, thermal decomposition, electrochemical deposition, and solution-phase processes have been introduced to prepare nano- or microscaled ZnO particles with various morphologies over the past decades.^{4,5} More recently, Wang et al. have reported the synthesis of ZnO nanorings by a solid–vapor process.⁶ Of these methods, the facile solution procedures may be the most simple and effective way to prepare well-crystallized materials at a relatively low temperature. Moreover, the advantages of solution-based methods have also involved the remarkable influence of organic additives on the size and morphology of the final products.

Many of the previously reported synthetic methods are limited to the formation of the preferred one-dimensional ZnO nanostructure due to its highly anisotropic growth character along the *c* axis. Therefore, the development of a morphologically controlled synthesis of ZnO nanocrystals is urgently needed to satisfy the requirements for exploring the potential applications of ZnO materials. Large-scale use will require the development of simple, low-cost approaches to the synthesis of inorganic functional nanomaterials.⁷ One such method is to grow ZnO nanostructures from an aqueous solution at low temperatures. Here, we developed a low-temperature, environmentally benign,

* Corresponding authors. E-mail: An-Wu.Xu@mpikg.mpg.de (A.-W.X.); coelfen@mpikg-golm.mpg.de (H.C.). Telephone: 49-331-5679505 (A.-W.X.). Fax: 49-331-5679502 (A.-W.X.).

[†] School of Chemistry and Chemical Engineering, Sun Yat-Sen University.

[‡] Max Planck Institute of Colloids and Interfaces, Department of Colloid Chemistry MPI Research Campus Golm.

solution-phase approach to fabricate ZnO nanorings, disks, and diskoidlike crystals in the presence of commonly available polymers as crystal growth modifiers. A possible growth mechanism of the ZnO nanostructures based on typical polymer–crystals interactions in a mild aqueous solution is also given.

Experimental Section

Preparation. All chemicals, hexamethylenetetramine, $\text{Zn}(\text{NO}_3)_2 \cdot 6\text{H}_2\text{O}$, and polymers (Aldrich) were of analytical grade and were used without further purification. In a typical procedure, 5 mL of 2 M $\text{Zn}(\text{NO}_3)_2 \cdot 6\text{H}_2\text{O}$, 5 mL of 2 M hexamethylenetetramine (HMT), 10 mL of 3 g/L polymer (polyacrylamide, PAM, M_w 10 000; carboxyl-modified PAM, PAM-COOH, M_w 200 000, carboxyl content 30 mol %, Aldrich) aqueous solution, and 80 mL of deionized water were added into a 150-mL beaker. The mixture solution became milky right away and was stirred for 5 min, then transferred into a 250-mL flask. The solution was heated to 70 °C in 30 min with refluxing, kept reacting for 5 h without stirring, and then air-cooled to room temperature. The resulting white products were thoroughly washed with water and dried at 60 °C in a vacuum oven for further characterization.

Characterization. Powder X-ray diffraction (XRD) patterns were recorded on a PDS 120 diffractometer (Nonius GmbH, Solingen) with Cu K α radiation ($\lambda = 1.542 \text{ \AA}$). SEM images were performed on a JEOL JEM-6330F microscope operating at 15 kV. Transmission electron microscopic (TEM) images were obtained on a Zeiss EM 912 Ω microscope operated at 200 kV. High-resolution transmission electron microscopic (HRTEM) images and the selected area electron diffraction (SAED) patterns were obtained on a JEOL-2010 microscope with an accelerating voltage of 200 kV. Energy-dispersive X-ray spectroscopy (EDS) was attached to the JEOL 2010. Sample grids were prepared by sonicating powdered samples in ethanol for 20 min and evaporating one drop of the suspension onto a carbon-coated, holey film supported on a copper grid for TEM measurements. The photoluminescence emission spectra were recorded with a F-4500 spectrophotometer equipped with a 150-W xenon lamp as the excitation source at room temperature. The modeling morphology and growth habit were simulated by the Cerius² software (Accelrys).

Results and Discussion

Polymer-controlled crystallization of ZnO crystals was carried out in a mild aqueous solution. The phase purity of the products obtained in the presence of polyacrylamide (PAM) was examined by X-ray diffraction (XRD) measurement performed on a Rigaku X-ray diffractometer with Cu K α radiation. All of the peaks of the XRD pattern in Figure 1 can be readily indexed to a pure hexagonal phase [space group: $P6_3mc$] of ZnO nanorings with calculated lattice constants $a = 3.248 \text{ \AA}$, $c = 5.197 \text{ \AA}$ (JCPDS 36-1451).

The morphology and structure of the products were examined with scanning electron microscopy (SEM). As shown in Figure 2, the ZnO products obtained in the presence of PAM consist almost entirely of uniform hexagonal ringlike structures with small aspect ratios (<1). These nanorings have outer diameters of 400–900 nm, inner diameters of 300–800 nm, wall thickness of 70–200 nm, and lengths ranging from 300 to 800 nm. The hexagonal cross-section of the outer shape and central hole is easily identified (the inset in Figure 2). A small portion of ZnO hexagonal nanodisks and irregularly shaped particles can also be observed, as shown in Figure 2. There was no change of

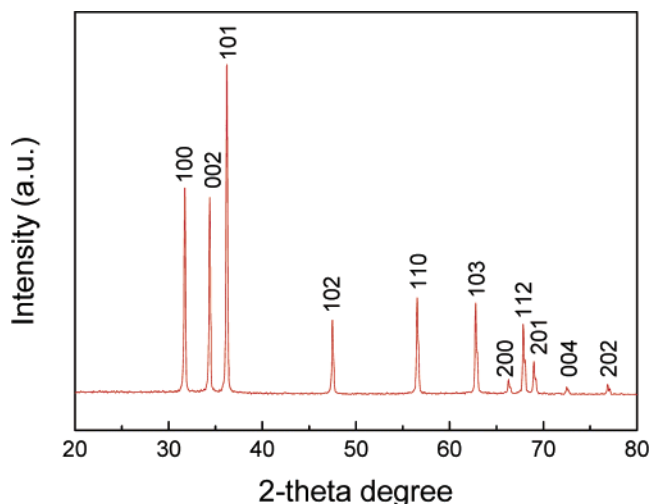


Figure 1. XRD pattern of the obtained ZnO nanorings grown for 5 h in the presence of polyacrylamide (PAM).

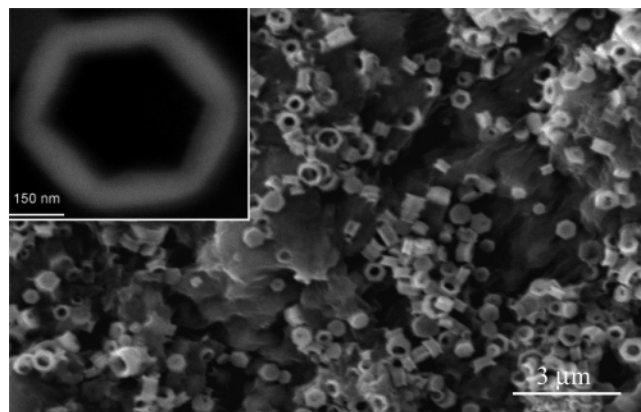


Figure 2. SEM images of the obtained ZnO nanorings grown for 5 h in the presence of PAM.

morphology for the sample grown in solution for 1 day in the presence of PAM.

The ringlike structure of the products was further examined with transmission electron microscopy (TEM) and high-resolution TEM (JEOL-2010 at 200 kV). Figure 3a shows the typical TEM image of a single ZnO nanoring with {001} top/bottom surfaces. Figure 3b shows a {001} zone-axis HRTEM image. Here the 6-fold symmetry and the 0.280 nm {100} lattice fringe in three directions are clearly resolved, and the nanoring normal is [001]. The selected area electron diffraction (SAED) pattern (Figure 3c) taken from this nanoring can be indexed as a hexagonal wurtzite ZnO single crystal recorded from the [001] zone axis. TEM observations show that each ring is a single crystal. Energy-dispersive X-ray spectroscopy (EDS) analysis shows that the sample contains Zn and O elements (Figure 4), confirming the composition of the product is ZnO.

It is obvious that the polymer plays an important role in the formation of these ringlike nanostructures. It is important to note that control experiments without PAM in the solution did not produce nanorings but elongated particles instead. When a smaller quantity of PAM (0.3 g/L) was added, compact ZnO rods with aspect ratio ca. 3 were obtained (Figure 5). With increase in PAM concentration, the aspect ratio was rapidly decreased. The result suggests that PAM molecules slowed crystal growth along the {001} orientation and, therefore, provided a simple approach to controlling the aspect ratio of the ZnO nanorings. The polymer molecules were selectively

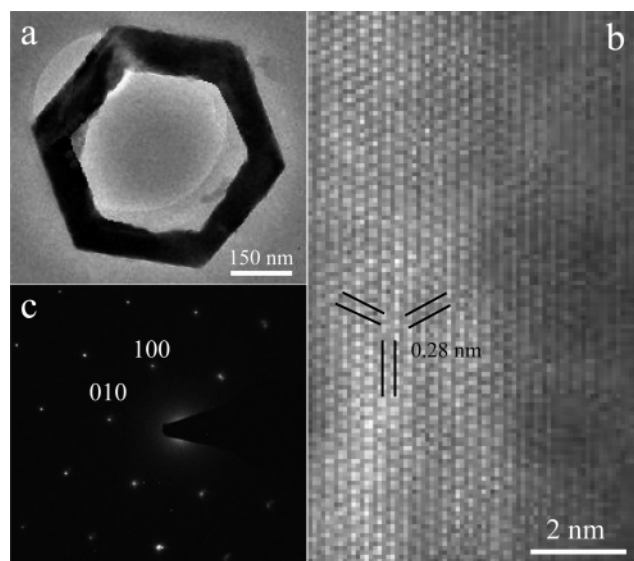


Figure 3. (a) TEM image of a single ZnO nanoring. (b) HRTEM image of the tube wall with clearly resolved lattice fringe of (100) planes ($d = 0.28$ nm). (c) Corresponding SAED pattern recorded from the [001] zone axis.

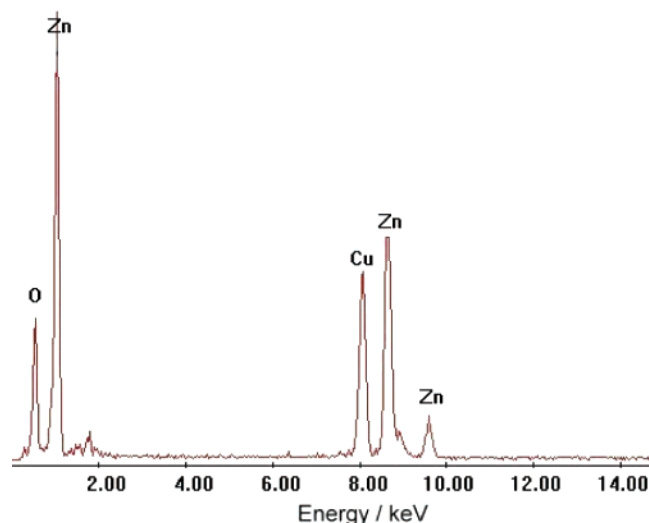


Figure 4. Energy-dispersive X-ray spectroscopy (EDS) spectrum of the obtained ZnO nanorings. Cu peak came from the TEM grid.

adsorbed on the basal plane, and crystal growth along the [001] direction was suppressed under these conditions, but the crystals were still able to grow sideways.

A ZnO crystal consists of a polar top face (001) consisting of tetrahedral zinc having a terminal OH ligand, a polar basal oxygen plane (00 $\bar{1}$), and a nonpolar plane (100) with C_{6v} symmetry. The low-symmetry, nonpolar (100) face is the most stable with its 3-fold coordinated atoms, while the polar faces are metastable. The large (001) polar surface is general energetically unfavorable unless the surface charge is compensated by a passivating agent. The velocities for growth under solution conditions are reported to $V_{001} > V_{010} > V_{100}$. In pure solutions, the most stable morphology is hexagonal, with the crystal elongated along the c -axis, as seen in the modeling of growth morphology by Cerius² software in Figure 6 (left).

This observation also goes well with earlier reports on polymer-controlled crystallization of ZnO crystals in the presence of diblock copolymers.^{8,9a} As compared to the large elongated crystals of the control sample, the polymers decreased the overall growth rate along the c direction (yielding shorter

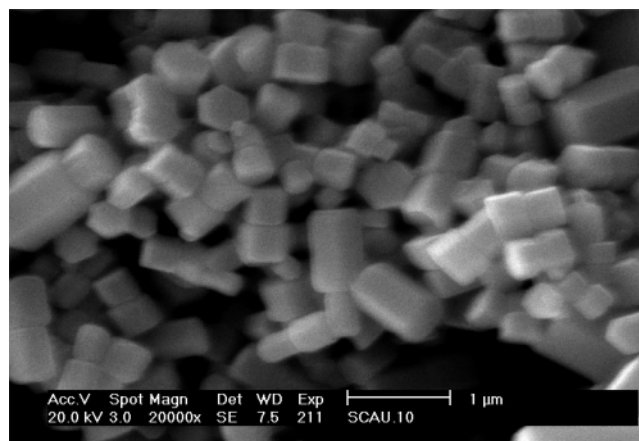


Figure 5. Typical SEM image of the obtained ZnO sample prepared in a low concentration of PAM (0.3 g/L).

crystals), but did not reduce the width significantly.^{9a} Taubert et al. showed that nearly rounded ZnO particles with a central grain boundary and a narrow size distribution were formed in the presence of PEO-*b*-PMAA.⁹ With the use of the stronger acidic poly(ethylene oxide-*block*-poly(styrene sulfonic acid)) (PEO-*b*-PSSH) copolymers, a lamellar intermediate precipitate was observed at the beginning, then this structure finally dissolved and hexagonal prismatic crystals were formed. A remarkable effect was found when a subsequent growth process gave rise to uniform “stack of pancakes” shaped ZnO crystals. The formation of a metastable intermediate and the release of the polymer from the side faces of the core crystals, as well as the selective adsorption on the (001) ZnO face, display a collective effect in the determination of such “stack of pancakes” morphology.^{9c} Recently, Tian et al. have used citrate ions to control the growth of the ZnO crystal and found that citrate ions adsorb to the (002) surface and force the crystal to grow into plates, but these plates have no holes.¹⁰

For polymer molecules anchored on nanocrystals in aqueous solution, binding and desorbing will form a dynamic equilibrium. When several hybrid nanocrystals meet, polymers bound to the primary nanocrystals can easily desorb and rearrange around the subsequently formed aggregates, favoring a rapid restructuring of the inner-coated inorganic crystals.¹¹ Nucleation and crystal growth will gradually occlude a polymer into the primarily formed crystals, forming organic–inorganic hybrid structures. TGA analysis suggests that the polymer was incorporated into the crystals. Experiences and observations made in the study of biomineralization are relevant.^{1–3} We propose that the formation of ZnO nanorings is driven by such restructuring of polymer–inorganic hybrid nanocrystallines during mineralization and the dissolution of nanocrystals during crystal growth based on the well-known Ostwald ripening process from the inner side toward the outside. The hybrid core part of the disk is composed of dense polymer stabilized primary nanocrystals, indicating that the density of defects at the center of the disk is highest. Therefore, the center part of the disk has a large tendency to dissolve and eventually lead to the formation of a hole at the center.¹¹

All of these observations allow the phrasing of a model explaining the unusual nanoring morphology. PAM contains in the side chain a large number of amide ligands that are able to coordinate with Zn^{2+} ions, that is, the otherwise just weakly exposed (001) face, leading to a lowering of surface energy and inhibition of growth along this direction. This polymer adsorption can, for nanostructures, only take place on one face (Figure 6, middle),¹² as otherwise, electroneutrality would be violated

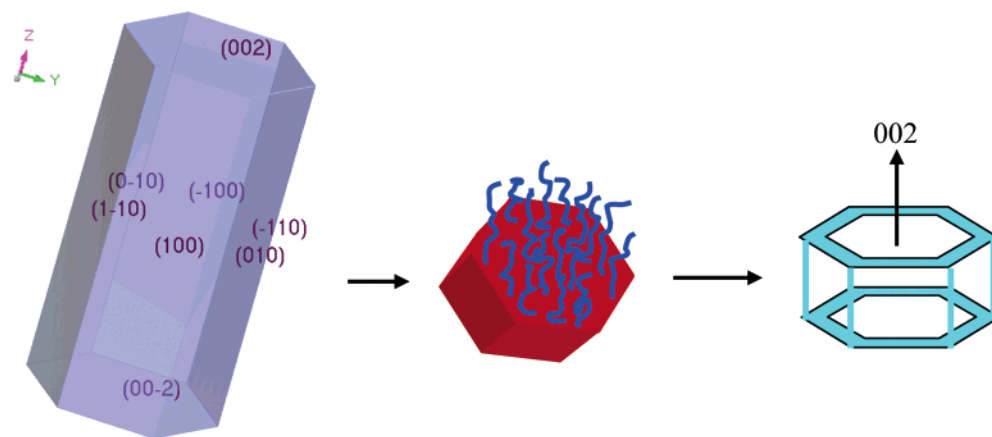


Figure 6. Modeling morphology and growth habit of ZnO crystals in the absence of any external influence (left, simulated with the Cerius² software), polymer adsorbed on (002) faces of ZnO (middle), and the final ZnO nanoring formation in the presence of PAM macromolecules (right).

(the counterface has to be negatively charged). Also, for a doubly positive structure, the internal repulsive Coulomb fields in the crystal would be too high. This structure, at least for the reversibly binding PAM, however, recrystallizes toward the final hollow single crystal (Figure 6, right). The formation of hollow crystal structures due to the metastability, sacrifice, and reconstitution of intermediary phases is a well-described phenomenon.^{3,13}

This model is also supported by some control experiments with another, more strongly binding derivative of PAM, which consequently also should be able to stabilize potential intermediates more efficiently. For that, carboxyl-functionalized PAM (PAM-COOH, carboxyl content 30 mol %) was also applied for ZnO crystallization. Figure 7 shows typical SEM and TEM images of the obtained ZnO disks grown for 5 h at a polymer concentration of 3 g/L, indicating these disklike crystals have uniform shape and size. In contrast to the sample obtained in the presence of PAM, no holes can be observed in the center of these disks. All crystals in the control samples exhibit a central grain boundary (Figure 7), similar to the structure reported by Wegner et al., using graft copolymers as additives.¹⁴ The back-to-back paired stacking of the two parts of the structure is a consequence of the natural asymmetry of the (001) and (00-1) faces counterbalances the dipolar fields of both substructures, and this was earlier assigned to twinning.^{9a} High-magnification SEM image and ED pattern (Figure 7b and e) shows that each disk consists of nanoparticles, which are presumably mesocrystals.¹²

Also for PAM-COOH, the hexagonal double cone (“diabolo”) is not stable and undergoes further ripening. When the reaction time was prolonged to 1 d, diskoidlike morphology was observed, as shown by the SEM image in Figure 8a. The high-magnification SEM image (Figure 8b) and TEM image, shown in Figure 8c, indicate that each diskoidlike crystal is formed, at least on its surface, from a large amount of ZnO nanoparticles. Electron diffraction (Figure 8d), however, shows that the sample, despite its curvature and rough surface appearance, is well crystallized. This unique diskoidlike morphology that is different from other shapes has not been reported for ZnO crystals to date and indicate that a different binding strength of the modifying polymer indeed seriously influences stability and shape of the final structures.

By comparison with microstructures formed in the presence of PAM-COOH, we believe that a similar structure indeed acts as the template sacrificed for the central hole of the nanorings formed in the presence of PAM. As PAM binds more weakly

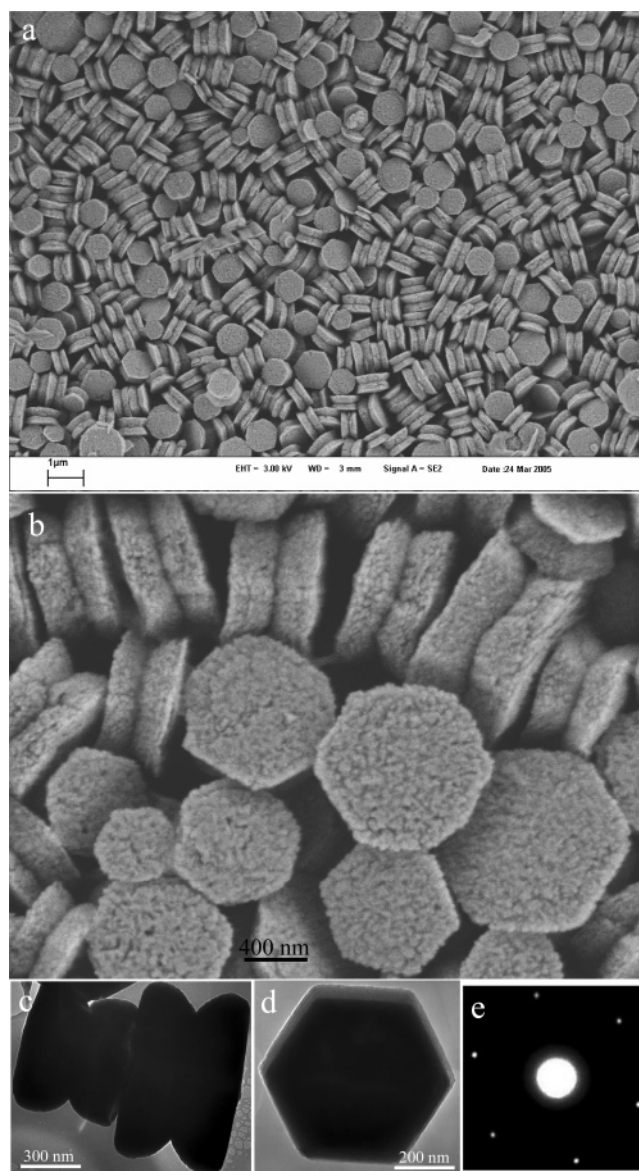


Figure 7. SEM (a, b), TEM images (c and d), and ED pattern (e) of the obtained ZnO disks in the presence of PAM-COOH grown for 5 h. Polymer concentration: 3 g/L.

and more dynamically than PAM-COOH, the lifetime of such high interface area structures controlled by PAM is shorter than

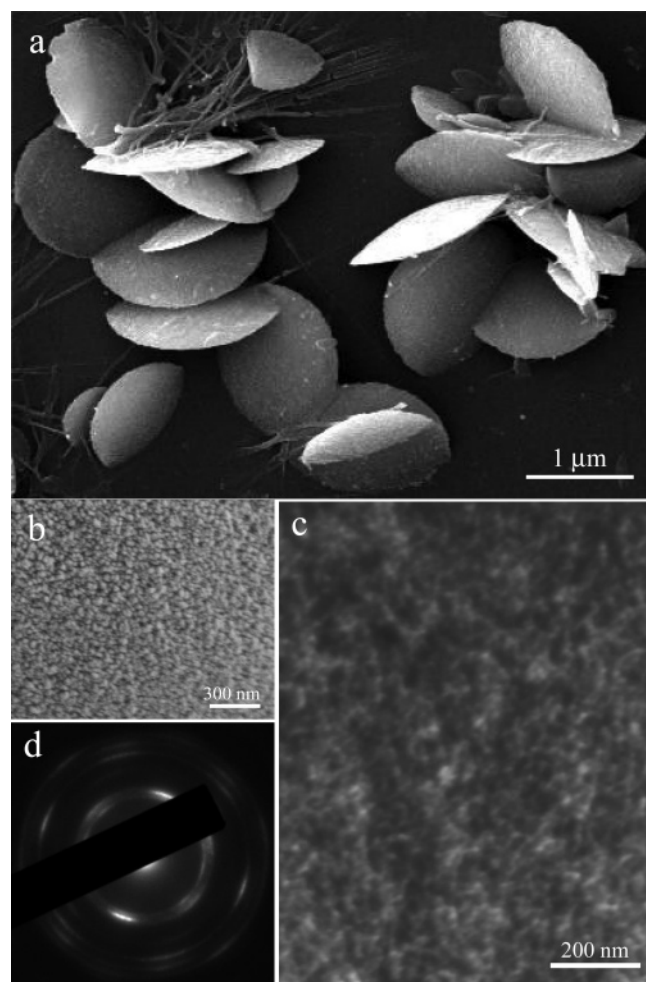


Figure 8. SEM images (a and b), TEM image (c), and ED pattern (d) of the obtained unique diskoidlike ZnO crystals in the presence of PAM-COOH grown for 1 day.

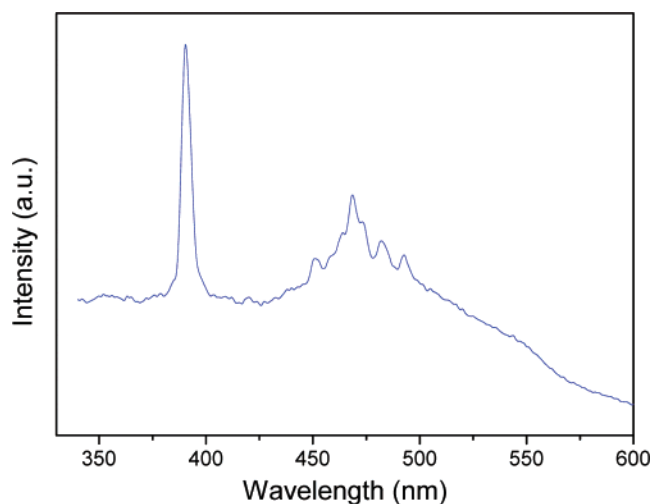


Figure 9. A room-temperature photoluminescence spectrum of the obtained ZnO nanorings recorded at an excitation wavelength of 325 nm.

that of structures controlled by PAM-COOH, and recrystallization toward the final single hollow crystal can occur.

A room-temperature PL spectrum of the obtained ZnO samples is shown in Figure 9. The strong sharp peak around 390 nm is attributed to the excitonic transitions.¹⁵ The weak emission peak centered at ~470 nm corresponds to the deep-

level or trap-state emission, which is known to be related to the structure defects.⁶ The full width at half-maximum (fwhm) of the UV emission of the obtained ZnO products is calculated to be approximately 8 nm, which is much narrower than that of commercial ZnO bulk crystals (~18 nm), indicating the obtained ZnO samples have a high optical property.¹⁶ The narrow fwhm confirms the uniformity and narrow size distribution of our synthesized ZnO crystals.

Conclusions

In conclusion, we have developed a mild aqueous solution route to obtain different morphologies of ZnO crystals with high crystallinity and uniform size and shape by polymer-controlled crystallization. Polymer-directed crystal growth and mediated self-assembly of nanoparticles can provide promising ways for rational synthesis of various ordered inorganic and inorganic-organic hybrid materials with complex form and structural speciality. The obtained hexagonal nanorings and diskoidlike crystals are new members in the family of ZnO nanostructures. The simplicity of mild solution process, cheapness, and availability of raw materials, without the need of catalyst, are advantages favoring the scaling-up of the novel method. Further work is needed to better understand the detailed mechanism involving a synergistic effect of the mutual interactions between functionalities of the polymers and inorganic species and the subsequent reconstruction in a “programmed” or “coded” way. The novel ZnO nanostructure may be used as building blocks for photonic and electronic nanodevice applications, e.g., in EUV applications or for “whispering gallery” mode microlasers.⁴

Acknowledgment. This work was supported by the National Natural Science Foundation of China (20371053) and the Guangdong Province NNSF (031574). A.-W. Xu thanks the Alexander von Humboldt Foundation for granting a research fellowship.

References and Notes

- (1) (a) Cölfen, H.; Mann, S. *Angew. Chem., Int. Ed.* **2003**, *42*, 2350. (b) Gower, L. B.; Odom, D. J. *J. Cryst. Growth* **2000**, *210*, 719. (c) Qi, L. M.; Cölfen, H.; Antonietti, M. *Angew. Chem., Int. Ed.* **2000**, *39*, 604. (d) Yu, S. H.; Cölfen, H.; Antonietti, M.; Hartmann, J. *Nano Lett.* **2003**, *3*, 379. (e) Kröger, N.; Deutzmann, R.; Sumper, M. *Science* **1999**, *286*, 1129. (f) Chan, C. S.; Stasio, G. D.; Welch, S. A.; Girasole, M.; Frazer, B. H.; Nesterova, M. V.; Fakra, S.; Banfield, J. F. *Science* **2004**, *303*, 1656. (g) Lahiri, J.; Xu, G. F.; Dabbs, D. M.; Yao, N.; Aksay, I. A.; Groves, J. T. *J. Am. Chem. Soc.* **1997**, *119*, 5449. (h) Orme, C. A.; Noy, A.; Wierzbicki, A.; McBride, M. T.; Grantham, M.; Teng, H. H.; Dove, P. M.; DeYoreo, J. J. *Nature* **2001**, *411*, 775.
- (2) (a) Mann, S. *Angew. Chem., Int. Ed.* **2000**, *39*, 3392. (b) Stupp, S. I.; Braun, P. V. *Science* **1997**, *277*, 1242.
- (3) Yu, S. H.; Cölfen, H. *J. Mater. Chem.* **2004**, *14*, 2124 and references therein.
- (4) (a) Pan, Z. W.; Dai, Z. R.; Wang, Z. L. *Science* **2001**, *291*, 1947. (b) Kong, X. Y.; Wang, Z. L. *Nano Lett.* **2003**, *3*, 1625. (c) Huang, M. H.; Mao, S.; Feick, H.; Yan, H.; Wu, Y.; Kind, H.; Weber, E.; Russo, R.; Yang, P. *Science* **2001**, *292*, 1897.
- (5) (a) Lao, J. Y.; Wen, J. G.; Ren, Z. F. *Nano Lett.* **2002**, *2*, 1287. (b) Hu, J. Q.; Li, Q.; Meng, X. M.; Lee, C. S.; Lee, S. T. *Chem. Mater.* **2003**, *15*, 305. (c) Wu, J. J.; Liu, S. C. *Adv. Mater.* **2002**, *14*, 215. (d) Xia, Y.; Yang, P.; Sun, Y.; Wu, Y.; Mayers, B.; Gates, B.; Yin, Y.; Kim, F.; Yan, H. *Adv. Mater.* **2003**, *15*, 353. (e) Vayssieres, L. *Adv. Mater.* **2003**, *15*, 464. (f) Zhang, J.; Sun, L. D.; Yin, J. L.; Su, H. L.; Liao, C. S.; Yan, C. H. *Chem. Mater.* **2002**, *14*, 4172. (g) Peterson, R. B.; Fields, C. L.; Gregg, B. A. *Langmuir* **2004**, *20*, 5114. (h) Liu, B.; Zeng, H. C. *J. Am. Chem. Soc.* **2003**, *125*, 4430. (i) Zhong, X. H.; Knoll, W. *Chem. Commun.* **2005**, 1158. (j) Govender, K.; Boyle, D. S.; Kenway, P. B.; O'Brien, P. J. *Mater. Chem.* **2004**, *14*, 2575 and references therein.
- (6) Kong, X. Y.; Ding, Y.; Yang, R.; Wang, Z. L. *Science* **2004**, *303*, 1348.

- (7) (a) Liu, B.; Yu, S. H.; Zhang, F.; Li, L. J.; Zhang, Q.; Ren, L.; Jiang, K. *J. Phys. Chem. B* **2004**, *108*, 4338. (b) Fang, Y. P.; Xu, A.-W.; Dong, W. F. *Small* **2005**, *1*, 967. (c) Xu, A.-W.; Fang, Y. P.; You, L. P.; Liu, H. Q. *J. Am. Chem. Soc.* **2003**, *125*, 1494. (d) Fang, Y. P.; Xu, A.-W.; Song, R. Q.; Zhang, H. X.; You, L. P.; Yu, J. C.; Liu, H. Q. *J. Am. Chem. Soc.* **2003**, *125*, 16025.
- (8) Öner, M.; Norwig, J.; Meyer, W. H.; Wegner, G. *Chem. Mater.* **1998**, *10*, 460.
- (9) (a) Taubert, A.; Palms, D.; Weiss, O.; Piccini, M. T.; Batchelder, D. N. *Chem. Mater.* **2002**, *14*, 2594. (b) Taubert, A.; Palms, D.; Glasser, G. *Langmuir* **2002**, *18*, 4488. (c) Taubert, A.; Kübel, C.; Martin, D. C. *J. Phys. Chem. B* **2003**, *107*, 2660.
- (10) Tian, Z. R.; Voigt, J. A.; Liu, J.; McKenzie, B.; McDermott, M. J.; Rodriguez, M. A.; Konishi, H.; Xu, H. *Nat. Mater.* **2003**, *2*, 821.
- (11) Li, F.; Ding, Y.; Gao, P. X.; Xin, X. Q.; Wang, Z. L. *Angew. Chem., Int. Ed.* **2004**, *43*, 5238.
- (12) (a) Wang, T. X.; Cölfen, H.; Antonietti, M. *J. Am. Chem. Soc.* **2005**, *127*, 3246. (b) Cölfen, H.; Antonietti, M. *Angew. Chem., Int. Ed.* **2005**, *44*, 5576.
- (13) Xu, A.-W.; Yu, Q.; Dong, W. F.; Antonietti, M.; Cölfen, H. *Adv. Mater.* **2005**, *17*, 2217.
- (14) Wegner, G.; Baum, P.; Müller, M.; Norwig, J.; Landfester, K. *Macromol. Symp.* **2001**, *175*, 349.
- (15) Yan, H.; He, R.; Pham, J.; Yang, P. *Adv. Mater.* **2003**, *15*, 402.
- (16) Geng, C.; Jiang, Y.; Yao, Y.; Meng, X.; Zapfen, J. A.; Lee, C. S.; Lifshitz, Y.; Lee, S. T. *Adv. Funct. Mater.* **2004**, *14*, 589.